



Strength weakening and its micromechanism in water–rock interaction, a short review in laboratory tests

Cun Zhang¹ · Qingsheng Bai² · Penghua Han¹ · Lei Wang¹ · Xiaojie Wang¹ · Fangtian Wang³

Received: 4 August 2022 / Revised: 20 August 2022 / Accepted: 16 January 2023
© The Author(s) 2023

Abstract

Water–rock interaction (WRI) is a topic of interest in geology and geotechnical engineering. Many geological hazards and engineering safety problems are severe under the WRI. This study focuses on the water weakening of rock strength and its influencing factors (water content, immersion time, and wetting–drying cycles). The strength of the rock mass decreases to varying degrees with water content, immersion time, and wetting–drying cycles depending on the rock mass type and mineral composition. The corresponding acoustic emission count and intensity and infrared radiation intensity also weaken accordingly. WRI enhances the plasticity of rock mass and reduces its brittleness. Various microscopic methods for studying the pore characterization and weakening mechanism of the WRI were compared and analyzed. Various methods should be adopted to study the pore evolution of WRI comprehensively. Microscopic methods are used to study the weakening mechanism of WRI. In future work, the mechanical parameters of rocks weakened under long-term water immersion (over years) should be considered, and more attention should be paid to how the laboratory scale is applied to the engineering scale.

Highlights

- (1) This paper reviews the water weakening on rock strength and its influencing factors.
- (2) Various microscopic methods for studying the pore characterization and weakening mechanism of WRI are compared and analyzed.
- (3) We study the weakening mechanism of WRIs using microscopic methods.
- (4) Future works on WRI laboratory tests were suggested.

Keywords Water–rock interaction · Weakening mechanism · Water content · Immersion time · Wetting–drying cycles · Microscopic methods

1 Introduction

Water–rock interactions (WRIs) are a topic of interest in geology and geotechnical engineering. Many physical and chemical reactions are involved in the WRI, including lubrication, precipitation, oxidation–reduction, and ion exchange. Many geological hazards and engineering failures, such as slope stability (Zhao et al. 2018c), reservoir dam stability (Ukpai 2021), rock bursting (Chen et al. 2019a; Ma et al 2022), karst collapse (Bai et al. 2013), and water inrush from mines and tunnels (Huang et al. 2016; Li et al. 2019b; Liu et al. 2022), are caused by the WRI. Analysis and interpretation of the influence of water on the mechanical behavior of rocks are based on the above problems. In recent years, many

✉ Cun Zhang
cumt-zc@cumt.edu.cn

✉ Penghua Han
18800149959@163.com

¹ School of Energy and Mining Engineering, China University of Mining and Technology (Beijing), Beijing 100083, China

² Institute of Geotechnics, TU Bergakademie Freiberg, Gustav-Zeuner-Straße 1, 09599 Freiberg, Germany

³ School of Mines, China University of Mining and Technology, Xuzhou 221116, China

studies have illustrated the effects of water on the mechanical characteristics of rocks. In general, the presence of water reduces the elastic modulus, compressive strength, cohesion, tensile strength, and rock brittleness (Baud et al. 2000; Erguler and Ulusay 2009; Zhou et al. 2017; Talesnick and Shehadeh 2007) and changes the fracture distribution and fragment shape after rock failure (Haberfield and Johnston 1990; Shen et al. 2020; Guha Roy et al. 2017; Kataoka et al. 2015). The water presence increases the pore water pressure in rock and soil mass, reducing the effective stress of rock and soil mass skeleton particles and changing the physical and mechanical parameters of the rock and soil mass. In addition, it is easy to cause the dissolution or change of mineral composition in rock, soil mass, and cement between grains to produce new mineral composition. The WRI effect will be greater if the water contains corrosive mineral components (Luo et al. 2021). For example, rocks with higher clay mineral content are more susceptible to water penetration (Verstrynge et al. 2014).

This short review focuses on the water weakening of rock strength and its influencing factors, such as the water content, immersion time, and wetting–drying cycles. On this

basis, the micromechanism of WRI and its corresponding research methods are addressed.

2 Water weakening characteristics and its influencing factors

Mechanical experiments combined with corresponding characterization methods are the primary methods used to study the weakening characteristics of the WRI. In conventional mechanical experiments (uniaxial and triaxial compression tests, Brazilian splitting tests, shear tests, point load tests, needle penetration tests, and Hopkins impact tests, as shown in Fig. 1), the shear, tensile, compressive, hardness, and dynamic load strengths can be obtained. In the test process, in addition to obtaining the stress–strain curves, acoustic emission (AE), infrared radiation temperature, digital image correlation (DIC), 3D laser scanning, and other methods are typically used to characterize the influence of the WRI (Fig. 1).

The weakening analysis of the WRI focuses on the influence of water content, immersion time, and wetting–drying

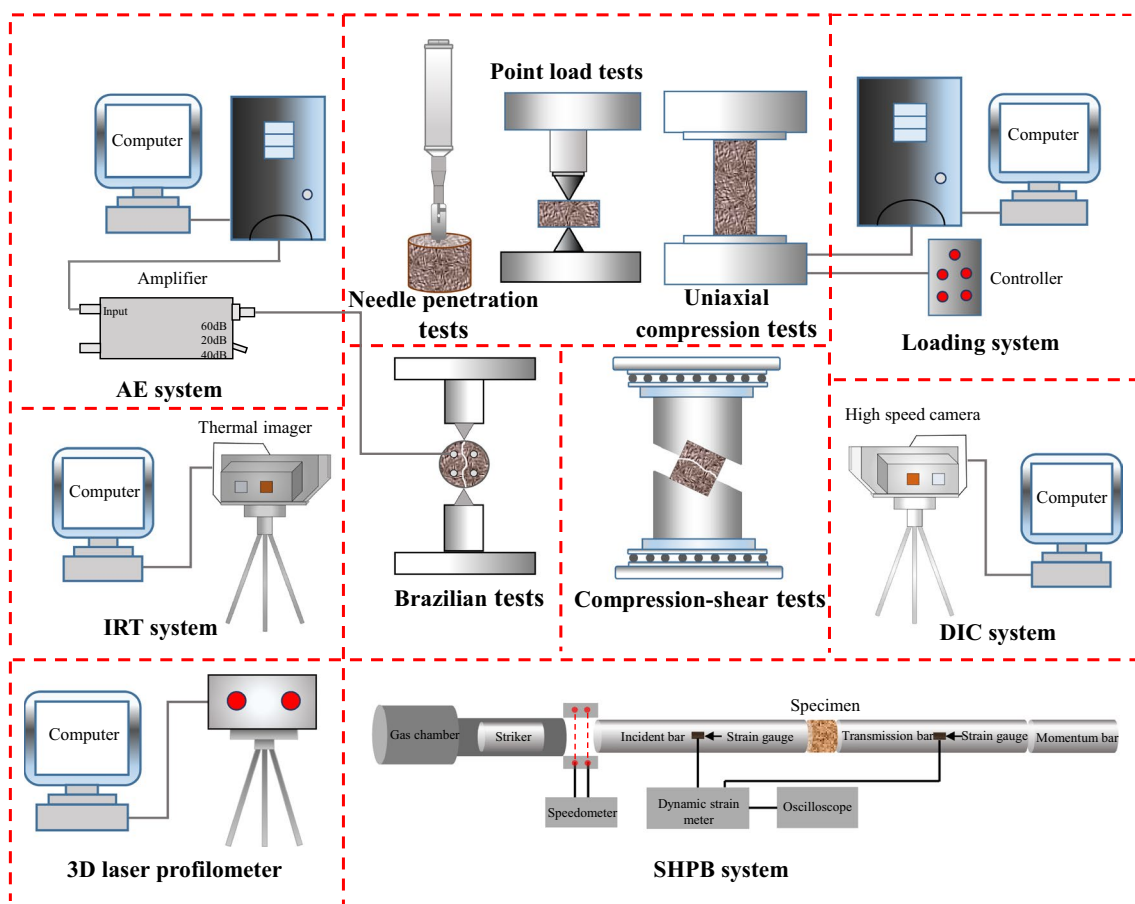


Fig. 1 WRI mechanics test and primary analysis

cycles on rock strength, as well as the corresponding AE and infrared radiation (IR) characteristics.

2.1 Water content

Water content can be divided into two aspects: (1) the water content state, including the dry state, natural water content state, and saturated water content state, and (2) the actual moisture content of the rock mass. There are two methods for preparing rock samples with different water contents: direct immersion in water and a non-destructive immersion method that places rock samples in a wet and closed environment to avoid the exchange or hydrochemical reaction between rock and water.

The compressive, shear, tensile strength, and elastic modulus decrease to varying degrees with the increasing water content, as summarized in Table 1. Among these, mudstone rocks have the highest water sensitivity. Granite and other hard rocks have the lowest sensitivity to water, and some rocks are unaffected by water. An increase in water content enhances the plasticity of the rock mass and reduces brittleness (Noël et al. 2021). Some quantitative relationships (fitting formula) between the mechanical parameters (σ_p , σ_c , σ_{tc} , τ , E , ν , c , ϕ , etc.) and water content are summarized in Table 1. In addition, the water content reduces the fracture toughness after rock failure (Zhou et al. 2018a, b; Hua et al. 2015).

AE describes the energy release characteristics of rocks during fracturing or cracking. Hard rocks typically accumulate more energy during loading and would release stronger AE signals during failure. As the water content increases, the cumulative and peak AE signals, high-frequency AE signals, AE signal differences, and AE signal distribution uniformity decrease (Li et al. 2019a, 2021b; Ranjith et al. 2008; Guo et al. 2018; Lin et al. 2019; Zhu et al. 2020; Liu et al. 2019). In addition, with an increase in water content, AE is concentrated in the fracture stage, and the fractal dimension decreases (Song et al. 2020; Kong et al. 2017, 2019). Wet rocks generally produce small fragments during failure, which decreases the fractal dimension, and irregular fractures occur during loading.

For the correlation between moisture content and IR, the average IR temperature (AIRT) generally increases with increasing load and depends on the state of the rock samples (wet or dry, damaged or not). Before the damage, wet rocks generally show a faster increase in the AIRT, whereas dry rocks would produce more increments in the AIRT during damage (Deng et al. 1997; Liu et al. 2010). However, in the entire loading process, the higher the water content, the greater the AIRT, and the smaller the AIRT fluctuation (Zhou et al. 2018c). Sun et al. (2021a) further showed that the applied stress controls IR; for example, the IR count (IRC) will simultaneously increase when the stress suddenly

drops. The water content reduces the stress due to water weakening. The above conclusions mainly rely on the uniaxial compression tests. Shear tests by Yao et al. (2020a) concluded that the IR characteristics were comparable to those of the uniaxial compression tests.

With increasing water content, the dynamic load strength and dissipated energy decreased, but the elastic modulus increased. The dynamic strength of saturated rocks is more sensitive to the strain rate than that of dry rocks. With an increase in the strain rate (43.9–156.7 per second), the water weakening effect decreases gradually (Cai et al. 2020b). Further, compared with the uniaxial compressive strength of dry rock samples, that of saturated rock increases with the loading rate in two stages: rapidly increases at low loading rates, and then decreases at high loading rates (Zhu et al. 2021).

2.2 Wetting–drying cycles

Many practical engineering problems involve wetting–drying (WD) cycles, such as rocks in exposed slopes, coastlines, and pumping reservoirs. Similar to preparing rock masses with different water contents, there are also two methods (free and pressure immersion method, air and oven (or heater) drying) for preparing rock samples experiencing WD cycles. A vacuum pressure condition is adopted to accelerate rock saturation when preparing rock immersion, whereas the free immersion method is performed under atmospheric pressure conditions. In the drying process, oven drying can accelerate the drying of rocks compared with air drying. Previous laboratory tests have shown that the WD cycle treatment has a significant impact on the mechanical and physical properties (A_w , P , PLI, SDI, K_{IC} , K_{IIC} , K_{eff} , V_p , σ_c , σ_t , E , c , ϕ , τ , σ_{cd} , E_d , T_c , R , and H) of the rock, as summarized in Table 2 (Liu and Zhang 2020; Momeni et al. 2017; Zhou et al. 2018b; Chen et al. 2019c; He et al. 2020; Huang et al. 2022).

Although the WD cycle treatment methods were different in these studies, consistent weakening characteristics were observed. With progressive WD cycles, the porosity and water absorption increased monotonically, whereas the other parameters in Table 2 generally decreased. The decrease in mechanical and physical parameters gradually diminished with the progression of WD cycles (Sun and Zhang 2019; Khanlari and Abdilor 2015; Huang et al. 2010; Fu et al. 2017; Zhao et al. 2018a; Gratchev et al. 2019; Yao et al. 2019b; Wu et al. 2020b; Cai et al. 2020a; Li et al. 2021c). For example, it was found that the first 10 WD cycles significantly impacted the rock's strength; there was no change (Zhao et al. 2021; Guo et al. 2021) in the following cycles. The fracture toughness and crack propagation were also affected by the WD cycle. The fracture energy and fraction coefficient decrease with WD cyclic treatment (Zhao et al. 2017b, c; Song et al. 2019; Ma et al. 2018). The rock's

Table 1 Summary of laboratory tests of the effect of different water contents on the physical and mechanical characteristics of coal and rock

Rock type (Region)	Water content	Experimental equipment	Mechanical parameters	Change trend with water content	References
Sandstone (Tennessee, USA)	<i>w</i> : Dry, saturated	TTA, SEM,	σ_{1c}	σ_{1c} decrease	Feucht and Logan (1990)
Coal (Ningxia, China)	<i>w</i> : 0%, 7.10%, 15.68%, 22.90%, 23.09%	CS tests, AE system, IRM system	c, φ, τ , Amplitude of the AIRT	$\varphi = 2.39e^{-0.17w} + 37.24$, $c = 0.371e^{-0.12w} + 0.8898$, $\tau = -0.543w + 3.7797$, the amplitude of the AIRT decrease	Yao et al. (2020a)
Granite, tuff, andesite (Fukushima, Japan)	Dry, saturated	UTS tests	$\sigma_c, \sigma_t, R_{UTS}, R_{UCS}$	σ_c and σ_t decrease, $R_{UTS} = 1.61R_{UCS}$	Hashiba and Fukui (2015)
Sandstone (Sichuan, China)	<i>w</i> : 0%, 1.03%, 2.04%, 3.14%	UCS tests, AE system, SEM	σ_c, E, ν	$\sigma_c = 80.604e^{-0.9044w} + 43.17$, $E = 20.451 - 4.7481w$, $\nu = 0.2 + 0.011e^{1.748w}$, $\epsilon_c = 0.1$	Li et al. (2021a, b, c)
Black sandstone (Sichuan, China)	<i>w</i> : 0%, 0.32%, 0.34%, 0.70%, 0.91%, 1.18%, 1.62%	UCS tests	σ_c, E, ν	$213w^2 - 0.2744w + 0.7216$	Tang (2018)
Coal (Heilongjiang, China)	Dry (0%), Natural (0.43%), Saturated (1.70%)	MTTA, AE system, SEM, HSVC	σ_{1c}, E , Cumulative AE counts, Cumulative AE energy	σ_{1c} and E decrease, Cumulative AE energy and counts decrease	Sun et al. (2016)
Coal (Henan, China)	<i>w</i> : 0%, 6.00%, 9.75%, 10.96%	UCS, AE system, MIP, XRD, SEM	σ_c, R_A, AF	RA increase, σ_c and AF decrease	Yao et al. (2019a, b)
Shale beams (Pennsylvania, USA)	Dry (0%), Saturated (%)	TPB, CT, AE system	σ_t	σ_t decrease	Lu et al. (2021)
Mudstone (Xinjiang, China)	<i>w</i> : 0%, 1.00%, 2.00%, 3.00%, 4.00%, 5.10%, 6.00%	UCS, UTS, SEM	$\sigma_c, \sigma_t, c, \sigma_{1c}, \epsilon_c$	$\sigma_c = 19.32e^{-0.52w} + 4.06$, $\sigma_t = 2.42e^{-0.44w} + 0.29$, $c = 5.22e^{-0.59w} + 1.63$, σ_{1c} decrease, ϵ_c decrease and then increase	Liu et al. (2021)
Sandstone (Shandong, China)	<i>w</i> : 0%, 0.8%, 1.6%, 2.4%, 3.2%	XRD, FJRE system	σ_c, E, D_c	$\sigma_c = 52.5416e^{-1.9_{115w}} + 37.6738$, $E = 5.9348e^{-1.5541w} + 7.5865$, $D_c = 0.6445 - 0.6445e^{-0.8253w}$	Sun et al. (2021a, b)
Tuff (Sapporo, Japan), Sandstone (Kushiro, Japan)	<i>w</i> : dry, saturated	XRD, NP	V_p, NPI	V_p and NPI decrease	Fujii et al. (2020)
Siltstone and gypsiferous rock (Alicante, Spain)	<i>w</i> : dry, saturated	UCS, XRD, MIP	ρ, σ_c, NPI, E	ρ increase, σ_c, E and NPI decrease, $\sigma_c = 0.13389NPI$ (Siltstone), $\sigma_c = 0.12559NPI$ (gypsiferous rock)	Rabat et al. (2020)
Sandstone (Shanxi, China)	<i>w</i> : 0%, 1.13%, 1.58%, 2.52%, 3.63%	UCS, SEM, XRD, Creep test	$\sigma_c, E, t_1, \epsilon'$	$\sigma_c = 44.600e^{-0.399w} + 66.6602$, $E = 5.640e^{-0.357w} + 13.426$, t_1 increase, ϵ' increase	Chen et al. (2021)
Clay-rich sandstone (Gansu, China)	<i>w</i> : 0.69%, 0.88%, 1.00%, 1.73%, 1.99%, 2.24%, 2.28%	XRD, SEM, MI test, SV test, SD test	E, h, H, V_p	h and V_p increase, E and H decrease	Azhar et al. (2020)

Table 1 (continued)

Rock type (Region)	Water content	Experimental equipment	Mechanical parameters	Change trend with water content	References
Red sandstone (Hunan, China)	ω : dry, saturated (3.40%)	SEM, UCS	$E, \sigma_c, t_1, \epsilon'$	$\sigma_c = 55.21e^{-0.7502\omega} + 51.6$ $E = 6.183e^{-0.6847\omega} + 10.62, t_1$ increase, ϵ' increase	Tang et al. (2018)
Coal (Shanxi, China)	ω : 0%, 2.37%, 3.78%, 5.29%	UCS, AE system	E, σ_c	$\sigma_c = -2.56\omega + 23.25$ $E = 1.05e^{-0.50\omega} + 0.72$	Yao et al. (2016)
Coal–rock combination (Shanxi, China)	ω : dry, natural, saturated	AE system, IRM system,	E, σ_c, ϵ_c	σ_c, E and ϵ_c decrease	Yao et al. (2020b)
Coal (Sichuan, China)	ω : dry, saturated	MTTA, CT, AE system	$E, \sigma_{te}, \epsilon_c, RA, AF$	σ_{te}, E, AF and ϵ_c decrease, RA increase	Liu et al. (2019)
Sandstone (China)	ω : 0%, 0.50%, 1.50%, 2.50%	UCS, IRM system	$\sigma_c, \epsilon_c, AIRC$	σ_c, ϵ_c decrease, AIRC increase	Sun et al. (2021a, b)
Red sandstone (China)	ω : natural (0.65%), saturated (2.37%)	UCS, MTTA, XRD,	E, V_p, σ_c	V_p increase, σ_c and E decrease	Luo (2020)
Marble, Limestone (Sichuan, China)	ω : Dry (0%), saturated (marble: 3.01%, limestone: 1.87%)	UCS, AE system, XRD	E, σ_c, H -type waveforms, L-type waveforms	σ_c and E decrease, H-type waveforms decrease, L-type waveforms increase	Zhu et al. (2021)
Red sandstone (Hunan, China)	ω : 0%, 0.70%, 1.60%, 2.60%, 3.50%, 4.60%, 4.70%	UCS, SEM, XRD	$\sigma_c, E, \epsilon', t_1$	$\sigma_c = 24.4e^{-0.55\omega} + 49.4$ $E = 3.4e^{-0.34\omega} + 7.4, \epsilon'$ increase, t_1 decrease	Yu et al. (2019)

Note: AE acoustic emission, CT computed tomography, NP needle penetration, CS compression shear, UCS unconfined tensile strength, UCS unconfined compression strength, MTTA modified true triaxial apparatus, FIRE five joint rheological experimental, TPB three-point bending, MI micro indentation, SV sonic velocity, SD slake durability, SEM scanning electron microscopy, ϵ_c Peak strain, HSWC high speed video camera, IRM infrared radiation monitoring, MIP mercury intrusion porosimetry, RA rise time divided by peak amplitude, AF counts divided by duration, ϕ friction angle, c cohesion, E Young's modulus, σ_1 tension strength, MPI needle penetration index, σ_c uniaxial compressive strength, σ_{te} triaxial compressive strength, τ shear strength, ν Poisson's ratio, ρ Density, V_p P-wave velocity, t_1 creep time-to-failure, ϵ' Minimum creep strain rate, h indenter depth, H hardness, AIRC average infrared radiation count, R_{UTS} reduction of uniaxial tension strength, R_{UCS} reduction of uniaxial compression strength

Table 2 Summary of laboratory test results of rock mechanical and physical properties with WD cycle treatment

Rock type	Sample size	Treatment methods		Cycle number	Test results	Reference
		Wetting	Drying			
Coal	CS ($\phi 50 \times 100$)	WW (24 h)	OD (95 °C/24 h) AD (20 °C/4 h)	10	A_w increase; σ_c , E decrease	Chen et al. (2019b)
Granite	CS ($\phi 50 \times 100$)	WW (24 h)	OD (105 °C/12 h)	60	σ_c , E decrease	Chen et al. (2019c)
Sandstone	CS ($\phi 50 \times 100$)	WW (24 h)	OD (105 °C/12 h)	20	σ_c , E , c , Φ decrease	Liu et al. (2018)
Granite	CS ($\phi 50 \times 100$)	WW (24 h)	OD (105 °C/12 h)	20	σ_c , E , c , Φ decrease	Qin et al. (2018)
Sandstone; mudstone	CS ($\phi 50 \times 100$)	WW (24 h)	OD (110 °C/12 h)	40	A_w increase; σ_c , E decrease	Huang et al. (2018)
Greywacke; Basalt	CS ($\phi 50 \times 50$)	WW (24 h)	OD (100 °C/12 h)	40	PLI, SDI decrease	Gratchev et al. (2019)
Weak muddy intercalation	CS ($\phi 61.8 \times 20$)	WW (24 h)	OD (40 °C/45 h)	6	τ , c decrease	He et al. (2020)
Sandstone	CS (Length to diameter ratio of 2.5 to 3.0)	WW (24 h)	OD (110 °C/12 h)	40	σ_c , decrease	Khanlari and Abdilor (2015)
Sandstone	CS ($\phi 25 \times 50$)	WW (24 h)	OD (80 °C/2 h)	50	T_c , σ_t , V_p decrease	Sunand Zhang (2019)
Ignimbrite	CS ($\phi 54 \times 108$)	WW (24 h)	OD (105 °C/12 h)	50	A_w P increase; V_p , σ_c , decrease	Özbek (2014)
Granitoid rocks	Rock pieces	WW (24 h)	OD (110 °C/24 h)	40	SID decrease	Momeni et al. (2017)
Sandstone	CCBD specimen	WW (48 h)	OD (105 °C/24 h)	7	K_{eff} , σ_t decrease	Hua et al. (2017)
Sandstone	CSTBD specimen	WW (48 h)	OD (105 °C/24 h)	7	K_{IIC} , decrease	Hua et al. (2016)
Sandstone	CCNBD specimen	WW (48 h)	OD (105 °C/24 h)	20	P increase; K_{IC} , K_{IIC} decrease	Dehestani et al. (2020)
Sandstone	CCBD specimen	WW (48 h)	OD (105 °C/24 h)	7	K_{IC} , σ_t decrease	Hua et al. (2015)
Mudstone	Rock pieces	WW (3 days)	AD (26 °C/24 h)	11	SID , decrease	Liu and Zhang (2020)
Sandstone	CS ($\phi 50 \times 100$)	WW (5 days)	OD (105 °C/12 h)	15	σ_c , E , V_p decrease	Huang et al. (2020a, b)
Sandstone	NSCB specimen	WW (25 °C/24 h)	AD (25 °C/6 days)	50	P increase; V_p , K_{IC} , decrease	Cai et al. (2020a)
Tuff	CS (L/D ratio of 2.5)	WW (15–24 °C/24 h)	OD (105 °C)	52	A_w P increase; σ_c , V_p , decrease	Topal and Sözmen (2003)
Sandstone	CS ($\phi 50 \times 25$)	WW (25 °C/24 h)	AD (25 °C/6 days)	50	A_w P increase; V_p , SDI , σ_t decrease	Zhou et al. (2018b)
Sandstone	CS ($\phi 50 \times 25/100$)	WW (25 °C/25 days)	OD (110 °C/24 h)	5	σ_c , σ_t , E , decrease	Yao et al. (2020c)
Granite	CS ($\phi 50 \times 25$)	WW (25 °C/10 h)	OD (50 °C/10 h)	100	R increase; H decrease	Zhao et al. (2020)
Sandstone	CS ($\phi 50 \times 50$)	WW (25 °C/48 h)	AD (25 °C)	50	A_w P increase; V_p , SDI , σ_{cd} , E_d decrease	Zhou et al. (2018a)
Iron ore	CS ($\phi 50 \times 100$)	GWW (8 h) WW (48 h)	AD (26 °C/7 days)	15	σ_c , E , V_p , decrease	Yang et al. (2018)
Sandstone	CS ($\phi 50 \times 100$)	GWW (6 h) WW (6 h)	OD (50 °C/12 h)	25	A_w increase; V_p , σ_c , E decrease	An et al. (2020)
Sandstone	CS ($\phi 50 \times 100$) CS ($\phi 50 \times 50$)	GWW (6 h) WW (12 h)	OD (50 °C/12 h) AD (48 h)	30	A_w , ϵ_c increase; σ_c , E , c , φ decrease	Li et al. (2021c)
Sandstone	CS ($\phi 50 \times 25$)	GWW (6 h) WW (18 h)	AD (3 days)	15	σ_t , decrease	Zhao et al. (2017b)
Mudstone	CS ($\phi 25 \times 50$)	WWV (–10 MPa/24 h)	OD (60 °C/24 h)	12	P increase; σ_c decrease	Zhao et al. (2018a)
Sandstone	CS ($\phi 50 \times 100$)	WWV (4 h) WW (44 h)	OD (45 °C/20 h); AD (4 h)	15	P increase; V_p , σ_c , c , decrease	Zhang et al. (2014)

Table 2 (continued)

Rock type	Sample size	Treatment methods		Cycle number	Test results	Reference
		Wetting	Drying			
Sandstone	CS	WWV (4 h) WW (44 h)	OD (105 °C/20 h); AD (4 h)	20	σ_c , E decrease	Xie et al. (2018)
Sandstone	CS ($\phi 50 \times 25/50$)	WWV (– 80 kPa/24 h)	OD (105 °C/24 h)	10	A_w increase; V_p , σ_t decrease	Liu et al. (2016)
Sandstone	SCB specimens; CS ($\phi 50 \times 50$)	WWV (– 80 MPa/24 h); WW (44 h)	OD (105 °C/24 h)	10	K_{IC} , σ_t decrease	Liang and Fu (2020)

Note: CS cylindrical sample, OD oven-dried; AD air-dried, GWW gradually water wetting (1/3 forward); WW/WWV water wetting without and with vacuum condition; BD Brazilian disk, NSCB/SCB notched/semi-circular bend; CCBD/CCNBD/CSTBD Brazilian disk with centrally-cracked/cracked chevron notch/cracked straight-through, R Surface roughness; T_c thermal conductivity; E_d dynamic Young's modulus; σ_{cd} dynamic compressive strength; σ_t tensile strength; K_{eff} effective fracture toughness; K_{IIC} mode II fracture toughness; K_{IC} mode I fracture toughness; SDI slake durability index; PLI point load index; P porosity; A_w water absorption

mineral composition has been found to be the main factor affecting the weakening of the WD cycle (Zhou et al. 2017; Tang et al. 2021).

2.3 Immersion time

The immersion time is more closely related to the actual field situation than the water content. Underground rock masses are occasionally immersed in water for months or years, and immersion time significantly affects rock strength (Bai et al. 2016). However, in most laboratory tests, the maximum immersion time is generally no longer than 1 year. The immersion time is currently limited because some rocks (especially those with strong hydrophilicity, such as mudstone) disintegrate after immersion for a short period (Azhar et al. 2020; Fujii et al. 2020). In addition, many studies have shown that some rocks do not weaken even after long-term immersion (Ai et al. 2021; Lyu et al. 2022).

As the immersion time increases, the mechanical parameters (σ_c , σ_t , E , c , ϕ , τ) of some rocks are weakened, their brittleness decreases, the failure mode becomes stable, and the roughness of the fracture planes increases (Zhu et al. 2020; Ma et al. 2021). The time-dependent immersion weakening varies for different rocks. For example, as the immersion time increases, the uniaxial compressive strength of coarse sandstones first decreases rapidly, then increases slightly, and finally decreases (Wu et al. 2020a). The uniaxial compressive strength and elastic modulus of argillaceous slates decrease with increasing immersion time, whereas Poisson's ratio remains roughly unchanged (Huang et al. 2020b).

2.4 Other WRI related factors

The chemical composition and water pressure play significant roles in WRI weakening. The mechanical parameters (σ_c , σ_t , E , c , ϕ , τ) of chemically treated samples generally

demonstrate more significant weakening compared with natural immersion conditions, especially for pre-fractured samples (Zhang et al. 2019; Gong et al. 2021). For example, the salts contained in water can gradually accumulate in the pore networks of rocks under wetting–drying cycles, which can cause rock deterioration (Jiang et al. 2022). The water immersion height also influences rock strength; the strength of partially presoaked specimens is lower than that of wholly presoaked specimens (Chen et al. 2021). Seepage water pressure enhances the deformation resistance of rock and affects rock strength. As seepage pressure increases, the stress thresholds for crack initiation and damage during rock compression decrease (Xiao et al. 2020; Zhong et al. 2019; Li et al. 2020b). Generally, studies on the WRI of rock mass cover various factors, and strength tests investigate the weakening characteristics under various immersion conditions to reflect engineering environments. Then, it is used to predict the degree of influence of the WRI on engineering scales.

3 Weakening mechanism and microscopic characterization

Many studies have shown that WRI is mainly the interaction between water and clay-related minerals in rocks, which changes the pore structure and further degrades their strength. Therefore, in addition to characterizing the macroscopic strength, investigating the internal microstructure is a valuable way to uncover WRI mechanisms. Microscopic observations include laser scanning confocal microscopy (LSCM) (An et al. 2020), polarizing microscopy (PM), scanning electron microscopy (SEM) (Dehestani et al. 2020; Zhang et al. 2014; Liu et al. 2018; Yang et al. 2018; Zhou et al. 2018b; Du et al. 2019), neutron radiography (NR), nuclear magnetic resonance (NMR) (Xie et al. 2018; Zhao et al. 2017a, 2018a,

b, 2019b), computed tomography (CT), and small angle X-ray scattering (SAXS) and other methods (Liu et al. 2016; Zhao et al. 2014, 2019a; Wang et al. 2021). The main application of the micro-observation techniques is shown in Fig. 2. The XRD pattern shown in Fig. 2 is typically used to investigate the hydrophilic mineral composition of the rocks.

The microinvestigation methods shown in Fig. 2 can be divided into three categories: SEM, PM, and LSCM. They are primarily used to observe the surface structure of a rock mass. SEM can be used to observe the mineral occurrence morphology, crystal morphology, surface morphology, and composition. However, the tested samples must be sprayed before SEM scanning; therefore, it is a destructive test.

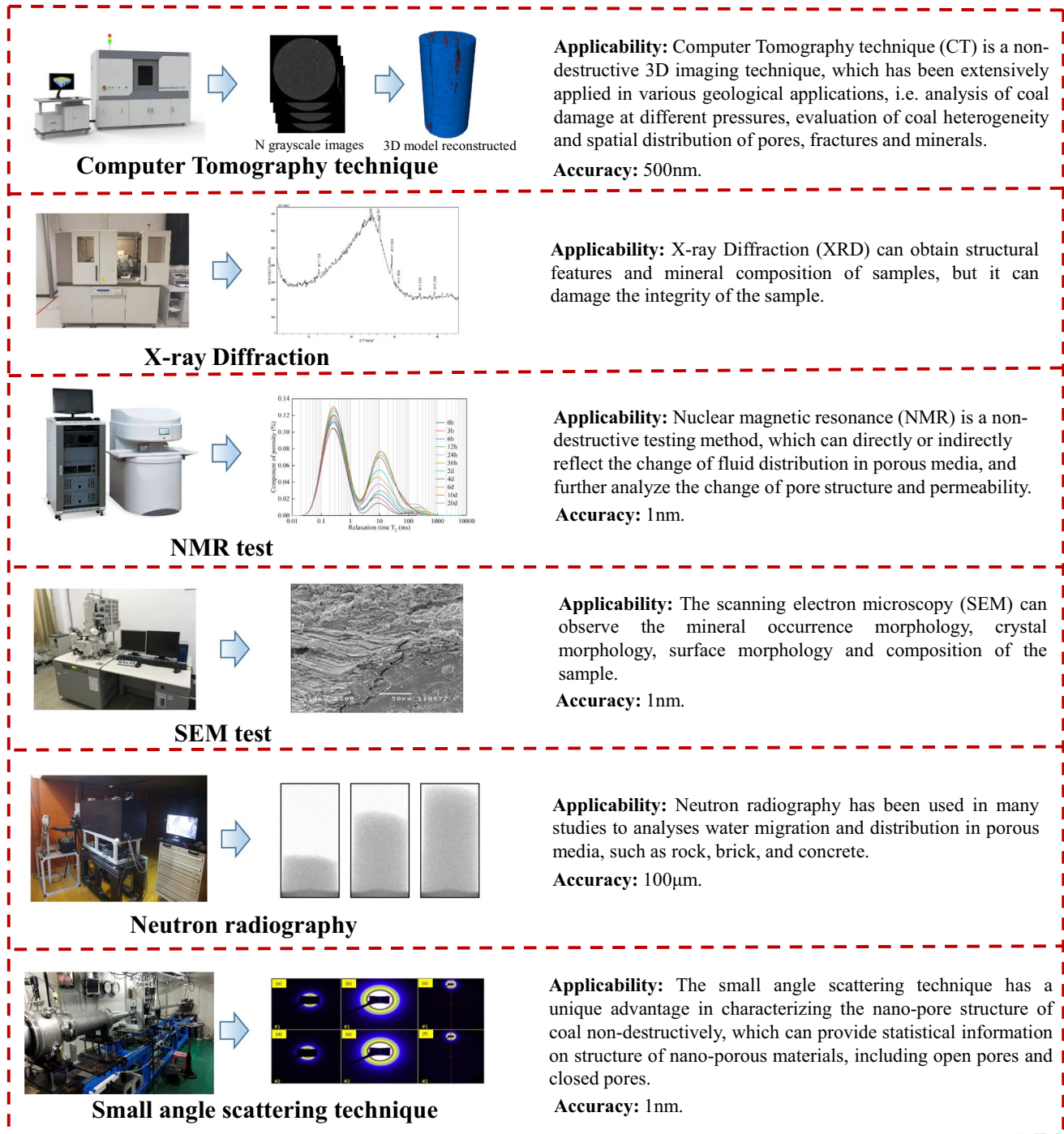


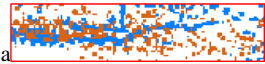

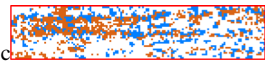
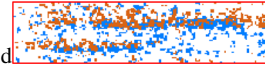
Fig. 2 Main characterization means of pore structure in WRI analysis

LSCM is mainly used for scanning the fracture surface. NMR and NR are mainly employed to judge pore structures and immersed liquids. The NMR is a non-destructive test that is widely used to characterize pore structures. However, NMR cannot be used to reconstruct a three-dimensional pore structure. CT, SAXS, and XRD are used for X-ray fluoroscopy, and the pore structure and mineral composition can be reconstructed with post-processing. CT is a non-destructive technique that can reconstruct pore and fracture structures in real time and is widely used to track pore and fracture evolutions during rock deformation. However, in the process of three-dimensional reconstruction of CT images, the division of pore fracture and mineral composition threshold is generally manually defined, which sometimes affects the accuracy of the reconstruction model.

Thus, various microcharacterization techniques are generally used for complementary analysis (Zhang et al. 2021; Ai et al. 2021). For example, NMR, XRD, and CT can be used to accurately reconstruct pore structures and mineral compositions (Fig. 3). Specifically, the mineral composition in the sample is first identified by XRD, such as clay mineral composition with strong hydrophilicity, and then the threshold is used during the reconstruction of CT images. Similarly, NMR can accurately provide the pore structure division threshold for CT reconstruction.

Based on the CT reconstruction method (Fig. 3), we reconstructed the pore structure and mineral composition model of the coal samples before and after water immersion. Table 3 shows the distribution of the pores with increased connectivity (blue) and reduced clay minerals (red) before and after immersion. The locations where the clay minerals are reduced coincide with the positions where the connectivity pores are increased. Further, the change in the pore structure in the sample during WRI is mainly caused by the

Table 3 Distribution map of pore and mineral changes

Pore and mineral distribution location	Coincidence ratio (%)
	59.82
	63.14
	65.38
	61.97

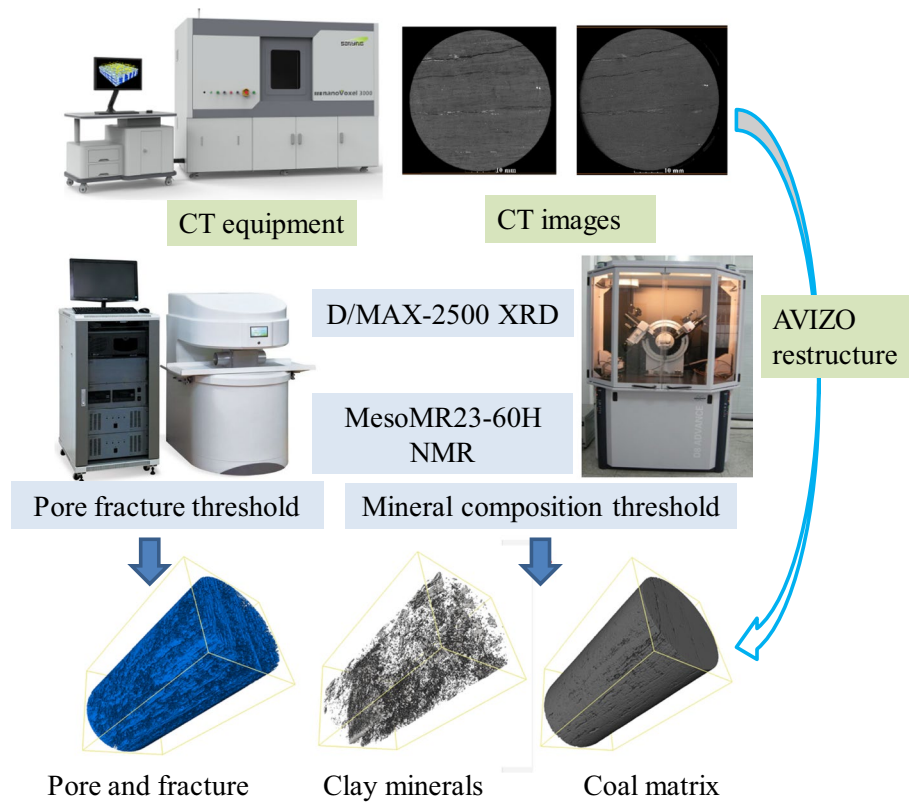


Fig. 3 Reconstruction process of "pore-fracture" dual structure of a coal sample

dissolution and expansion of hydrophilic mineral components (Azhar et al. 2020; Huanget al. 2020b; Liu et al. 2021).

Currently, five mechanisms for rock strength weakening caused by water immersion have been proposed: (1) expansion and dissolution of clay minerals, (2) reduction of capillary tension, (3) increase in pore pressure, (4) reduction of fracture energy, and (5) weakening of intergranular cohesion and friction (Zhu et al. 2020; Li et al. 2020a). By comparing the CT images before and after immersion (Fig. 4), the internal damage process caused by the WRI can be observed. Figure 4a and b show the CT images at the same position before and after immersion. The darkening of the greyscales in the CT images indicates an increase in damage and a decrease in density. Therefore, pre-existing weaknesses are displayed in darker colors. As shown in Fig. 4a, there are apparent darker parts (weaknesses) in the dry sample because coal is a typical porous medium with a large number of pore structures (connected pores and isolated pores) and fracture structures (Yao et al. 2019a). After immersion, the size and aperture of the internal fractures in the coal sample increased, and cleats between beddings gradually developed with water degradation. Fracture structures have better connectivity and higher permeability, forming the main flow channels of the fluid medium; meanwhile, clay minerals near the fractures are dissolved in water. In addition, water weakens the intergranular bonding of pre-existing weaknesses, and the development of fractures and pores (connected pores) increases the contact area between water and coal, resulting in the appearance of cleats between beds. For the rock samples, water mainly weakened the cementation between the crystals (Fig. 4d). The stress and energy required for failure along the fractures and cleats are significantly lower than those required for the direct penetration of the coal matrix and rock crystals; therefore, the higher the water content, the smaller the rock strength and the weaker the AE signal (Fig. 4) (Deng et al. 2021; Li et al. 2021a, b; Miao et al. 2021).

4 Conclusions and prospect

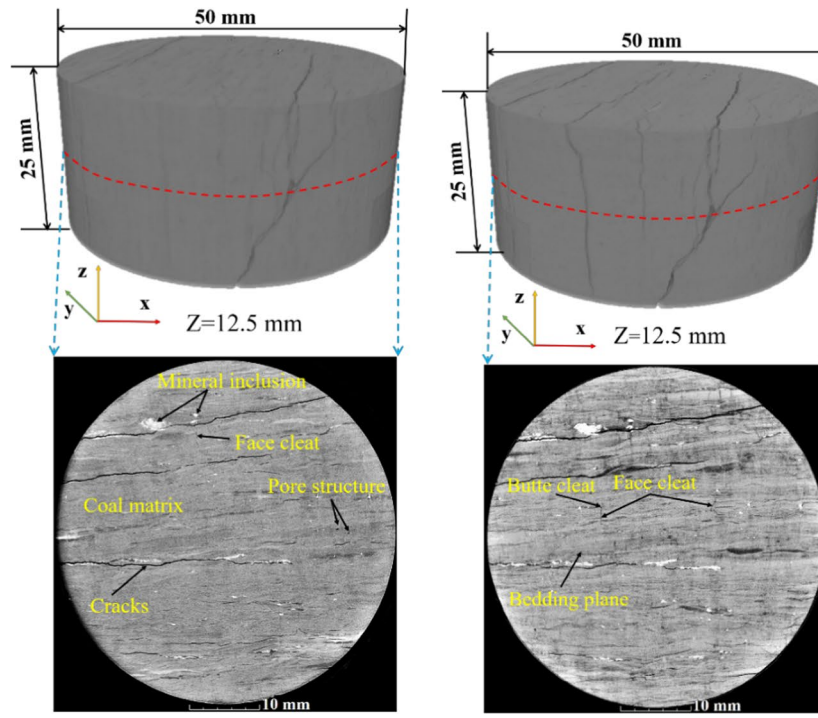
Research on the water weakening of rock masses mainly focuses on the effects of water content, water immersion time, and cyclic water immersion. The strength–weakening degree is characterized by uniaxial and triaxial strength, shear strength, tensile strength, point load, penetration, etc. AE and IR methods are typically used to study the fracture and energy characteristics during loading under WRI. The strength of the rock mass decreases to varying degrees with water content, immersion time, and WD cycles and is related to the type of rock mass and mineral composition. Generally, the strength decreases exponentially with an increase in water content. The previous several WD cycles have a significant impact on the strength of the rock mass and have

little effect on the progression of WD cycles. The degree of rock weakening gradually decreases with an increase in the immersion time. The corresponding AE count, intensity, and IR intensity also weaken accordingly. The WRI enhances the plasticity of rocks and reduces their brittleness.

Various microscopic methods have been used to study pore characterization and the weakening mechanism of WRI. SEM can qualitatively observe the fracture structure and mineral composition of the rock mass, but it is impossible to directly compare the porosity before and after water immersion owing to gold spraying during observation. NMR can quantitatively determine the porosity and pore size distribution and is a non-destructive test technique, making it possible to compare the pore size changes before and after immersion. CT scanning combined with corresponding reconstruction algorithms can quantitatively compare the changes in pore structure and mineral composition before and after immersion. However, the threshold division in CT image reconstruction is significant and directly affects the accuracy of the analysis. Thus, various micro-methods can be used to study the evolution of pore structure changes under WRI.

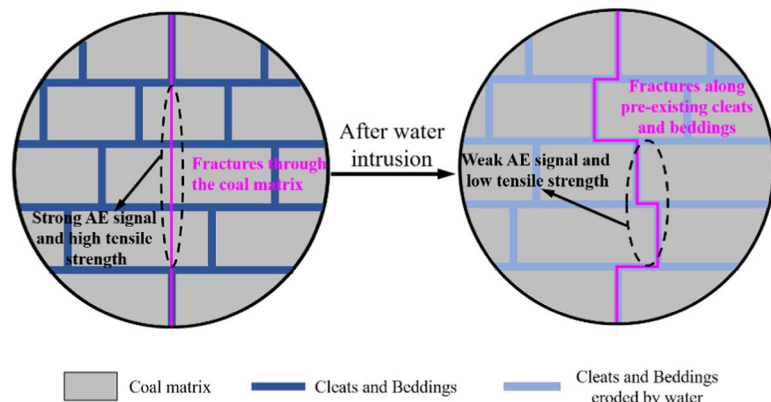
In the WRI weakening mechanism, the clay minerals in the rock mass dissolve in water, which expands the pore structures, increases the connected pores, further expands the primary fractures, and consequently increases the porosity and permeability. At the same time, the presence of water weakens the cementation strength near the primary fractures, making it easier to expand the splitting fracture along the joint surfaces. All these weakening processes lead to a decrease in rock strength and AE intensity.

Currently, studies on both the physical and mechanical properties and the weakening mechanism of WRI are relatively mature. Targeted experiments can only be carried out for special rock masses (different mineral compositions) or water environments (different water chemical compositions) in on-site engineering (water influence conditions). On this basis, the corresponding mechanical test modes (tension, compression, shear, or other tests), water influencing factors (moisture content, wetting–drying cycles, immersion time, etc.) and macro (AE, AIRT, etc.) and micro (SEM, NMR, CT, etc.) characterization methods can be considered. Thus, more attention should be paid to how laboratory-scale tests can be applied in engineering scale practice. Therefore, some qualitative conclusions must be transformed into quantitative models, which can then be applied to field engineering problems through numerical simulations. In addition, when investigating the effect of the immersion time, most laboratory tests are applied for less than half a year; however, long-term water immersion (even hundreds of years) problems generally occur. The weakening mechanism of WRI in rocks can also be explained using the changes in water immersion chemical ions and components.

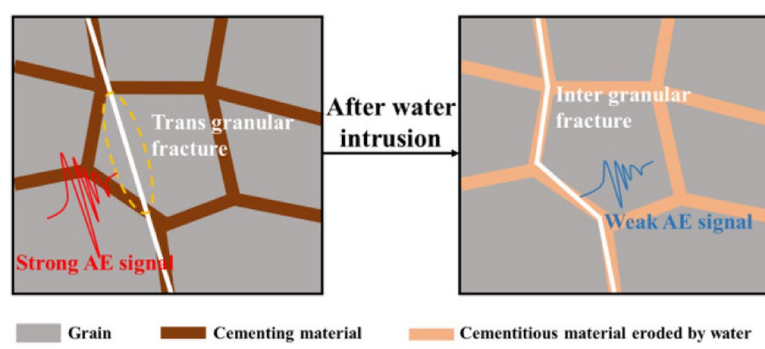


(a) Dry coal

(b) Saturated coal



(c) Coal-weakening mechanism



(d) Rock weakening mechanism

Fig. 4 CT images of a coal sample before and after water immersion. **a** Dry sample **b** Saturated sample **c** Coal-weakening mechanism and **d** Rock weakening mechanism

Acknowledgements Financial support for this work was provided by the National Natural Science Foundation of China (52104155), Natural Science Foundation of Beijing (8212032), and Fundamental Research Funds for the Central Universities (2023YQNY).

Author contributions CZ, QB, and PH drafted the manuscript. LW, XW, and FW participated in the drawing of figures in the paper. All authors approved the final manuscript for publication.

Data availability statement Some or all the data, models, or codes that support the findings of this study are available from the corresponding author upon reasonable request.

Declarations

Conflict of interest The authors declare no conflicts of interest regarding the publication of this article.

Open Access This article is licensed under a Creative Commons Attribution 4.0 International License, which permits use, sharing, adaptation, distribution and reproduction in any medium or format, as long as you give appropriate credit to the original author(s) and the source, provide a link to the Creative Commons licence, and indicate if changes were made. The images or other third party material in this article are included in the article's Creative Commons licence, unless indicated otherwise in a credit line to the material. If material is not included in the article's Creative Commons licence and your intended use is not permitted by statutory regulation or exceeds the permitted use, you will need to obtain permission directly from the copyright holder. To view a copy of this licence, visit <http://creativecommons.org/licenses/by/4.0/>.

References

- Ai T, Wu S, Zhang R, Gao M, Zhou J, Xie J, Zhang Z (2021) Changes in the structure and mechanical properties of a typical coal induced by water immersion. *Int J Rock Mech Min Sci* 138:104597
- An W, Wang L, Chen H (2020) Mechanical properties of weathered feldspar sandstone after experiencing dry–wet cycles. *Adv Mater Sci Eng*. <https://doi.org/10.1155/2020/6268945>
- Azhar MU, Zhou H, Yang F, Younis A, Lu X, Fang H, Geng Y (2020) Water-induced softening behavior of clay-rich sandstone in Lanzhou Water Supply Project, China. *J Rock Mech Geotech Eng* 12(3):557–570
- Bai H, Ma D, Chen Z (2013) Mechanical behavior of groundwater seepage in karst collapse pillars. *Eng Geol* 164:101–106
- Bai Q, Tu S, Zhang C, Zhu D (2016) Discrete element modeling of progressive failure in a wide coal roadway from water-rich roofs. *Int J Coal Geol* 167:215–229
- Baud P, Zhu W, Wong T (2000) Failure mode and weakening effect of water on sandstone. *J Geophys Res Solid Earth* 105(B7):16371–16389
- Cai X, Zhou Z, Tan L, Zang H, Song Z (2020a) Fracture behavior and damage mechanisms of sandstone subjected to wetting–drying cycles. *Eng Fract Mech* 234:107109
- Cai X, Zhou Z, Zang H, Song Z (2020b) Water saturation effects on dynamic behavior and microstructure damage of sandstone: phenomena and mechanisms. *Eng Geol* 276:105760
- Chen G, Li T, Wang W, Zhu Z, Chen Z, Tang O (2019a) Weakening effects of the presence of water on the brittleness of hard sandstone. *Bull Eng Geol Environ* 78(3):1471–1483
- Chen S, Jiang T, Wang H, Feng F, Yin D, Li X (2019b) Influence of cyclic wetting–drying on the mechanical strength characteristics of coal samples: a laboratory-scale study. *Energy Sci Eng* 7(6):3020–3037
- Chen X, He P, Qin Z (2019c) Strength Weakening and energy mechanism of rocks subjected to wet–dry cycles. *Geotech Geol Eng* 37(5):3915–3923
- Chen P, Tang S, Liang X, Zhang Y, Tang C (2021) The influence of immersed water level on the short-and long-term mechanical behavior of sandstone. *Int J Rock Mech Min Sci* 138:104631
- Dehestani A, Hosseini M, Beydokhti AT (2020) Effect of wetting–drying cycles on mode I and mode II fracture toughness of sandstone in natural (pH= 7) and acidic (pH= 3) environments. *Theor Appl Fract Mech* 107:102512
- Deng MD, Fang Z, Liu X (1997) Research on the action of water in the infrared radiation of the rocks. *Earthq Res China* 13(3):288–296
- Deng H, Qi Y, Li J, Jiang Q, Eleyas A, Li X (2021) Degradation mechanism of intermittent jointed sandstone under water–rock interaction. *Chin J Geotech Eng* 43(4):634–643
- Du B, Bai H, Wu G (2019) Dynamic compression properties and deterioration of red-sandstone subject to cyclic wet–dry treatment. *Adv Civ Eng* 2019:1–10
- Erguler ZA, Ulusay R (2009) Water-induced variations in mechanical properties of clay-bearing rocks. *Int J Rock Mech Min Sci* 46(2):355–370
- Feucht LJ, Logan JM (1990) Effects of chemically active solutions on shearing behavior of a sandstone. *Tectonophysics* 175(1–3):159–176
- Fu Y, Wang Z, Liu X, Yuan W, Miao L, Liu J, Dun Z (2017) Meso damage evolution characteristics and macro degradation of sandstone under wetting–drying cycles. *Chin J Geotech Eng* 12(4):1653–1661
- Fujii Y, Saito S, Oshima T, Kodama JI, Fukuda D, Sakata S, Dassanayake AB (2020) Complete slaking collapse of dike sandstones by fresh water and prevention of the collapse by salt water. *Int J Rock Mech Min Sci* 131:104378
- Gong C, Wang W, Shao J, Wang R, Feng X (2021) Effect of water chemical corrosion on mechanical properties and failure modes of pre-fissured sandstone under uniaxial compression. *Acta Geotech* 16(4):1083–1099
- Gratchev I, Pathiranagei SV, Kim DH (2019) Strength properties of fresh and weathered rocks subjected to wetting–drying cycles. *Geomech Geophys Geo-Energy Geo-Resour* 5(3):211–221
- Guha Roy D, Singh TN, Kodikara J, Das R (2017) Effect of water saturation on the fracture and mechanical properties of sedimentary rocks. *Rock Mech Rock Eng* 50(10):2585–2600
- Guo J, Feng GR, Qi T, Wang P, Yang J, Li Z, Wang Z (2018) Dynamic mechanical behavior of dry and water saturated igneous rock with acoustic emission monitoring. *Shock Vib* 2018:1–15
- Guo P, Gu J, Su Y, Wang J, Ding Z (2021) Effect of cyclic wetting–drying on tensile mechanical behavior and microstructure of clay-bearing sandstone. *Int J Coal Sci Technol* 8(5):956–968
- Haberfield CM, Johnston IW (1990) Determination of the fracture toughness of a saturated soft rock. *Can Geotech J* 27(3):276–284
- Hashiba K, Fukui K (2015) Effect of water on the deformation and failure of rock in uniaxial tension. *Rock Mech Rock Eng* 48(5):1751–1761
- He L, Yu J, Hu Q, Cai Q, Qu M, He T (2020) Study on crack propagation and shear behavior of weak muddy intercalations submitted to wetting–drying cycles. *Bull Eng Geol Environ* 79(9):4873–4889
- Hua W, Dong S, Li Y, Xu J, Wang Q (2015) The influence of cyclic wetting and drying on the fracture toughness of sandstone. *Int J Rock Mech Min Sci* 100(78):331–335

- Hua W, Dong S, Li Y, Wang Q (2016) Effect of cyclic wetting and drying on the pure mode II fracture toughness of sandstone. *Eng Fract Mech* 153:143–150
- Hua W, Dong S, Peng F, Li K, Wang Q (2017) Experimental investigation on the effect of wetting–drying cycles on mixed mode fracture toughness of sandstone. *Int J Rock Mech Min Sci* 93:242–249
- Huang S, Xia K, Yan F, Feng X (2010) An experimental study of the rate dependence of tensile strength softening of Longyou sandstone. *Rock Mech Rock Eng* 43(6):677–683
- Huang Z, Jiang Z, Zhu S, Wu X, Yang L, Guan Y (2016) Influence of structure and water pressure on the hydraulic conductivity of the rock mass around underground excavations. *Eng Geol* 202:74–84
- Huang S, Wang J, Qiu Z, Kang K (2018) Effects of cyclic wetting–drying conditions on elastic modulus and compressive strength of sandstone and mudstone. *Processes* 6(12):234
- Huang X, Pang J, Liu G, Chen Y (2020a) Experimental study on physicomaterial properties of deep sandstone by coupling of dry–wet cycles and acidic environment. *Adv Civ Eng* 2020:1–17
- Huang Z, Zuo Q, Wu L, Chen F, Hu S, Zhu S (2020b) Nonlinear softening mechanism of argillaceous slate under water–rock interaction. *Rock Soil Mech* 41(9):2931–2942
- Huang X, Pang J, Zou J (2022) Study on the effect of dry–wet cycles on dynamic mechanical properties of sandstone under sulfuric acid solution. *Rock Mech Rock Eng* 55(3):1253–1269
- Jiang X, Li C, Zhou JQ, Zhang Z, Yao W, Chen W, Liu HB (2022) Salt-induced structure damage and permeability enhancement of Three Gorges Reservoir sandstone under wetting–drying cycles. *Int J Rock Mech Min Sci* 153:105100
- Kataoka M, Obara Y, Kuruppu M (2015) Estimation of fracture toughness of anisotropic rocks by semi-circular bend (SCB) tests under water vapor pressure. *Rock Mech Rock Eng* 48(4):1353–1367
- Khanlari G, Abdilor Y (2015) Influence of wet–dry, freeze–thaw, and heat–cool cycles on the physical and mechanical properties of Upper Red sandstones in central Iran. *Bull Eng Geol Environ* 74(4):1287–1300
- Kong X, Wang E, He X, Li Z, Li D, Liu Q (2017) Multifractal characteristics and acoustic emission of coal with joints under uniaxial loading. *Fractals Complex Geom Patterns Scaling Nat Soc* 25(05):1750045
- Kong X, Wang E, Li S, Lin H, Xiao P, Zhang K (2019) Fractals and chaos characteristics of acoustic emission energy about gas-bearing coal during loaded failure. *Fractals Complex Geom Patterns Scaling Nat Soc* 27(05):1950072
- Li H, Shen R, Li D, Jia H, Li T, Chen T, Hou Z (2019a) Acoustic emission multi-parameter analysis of dry and saturated sandstone with cracks under uniaxial compression. *Energies* 12(10):1959
- Li S, Gao C, Zhou Z, Li L, Wang M, Yuan Y, Wang J (2019b) Analysis on the precursor information of water inrush in karst tunnels: a true triaxial model test study. *Rock Mech Rock Eng* 52(2):373–384
- Li H, Shen R, Wang E, Li D, Li T, Chen T, Hou Z (2020a) Effect of water on the time-frequency characteristics of electromagnetic radiation during sandstone deformation and fracturing. *Eng Geol* 265:105451
- Li Z, Xiong Z, Chen H, Lu H, Huang M, Ma C, Liu Y (2020b) Analysis of stress–strain relationship of brittle rock containing microcracks under water pressure. *Bull Eng Geol Environ* 79(4):1909–1918
- Li E, Feng J, Zhang L, Zhang H, Zhu T (2021a) Brazilian tests on layered carbonaceous slate under water–rock interaction and weathering. *Chin J Geotech Eng* 43(2):329–337
- Li H, Qiao Y, Shen R, He M, Cheng T, Xiao Y, Tang J (2021b) Effect of water on mechanical behavior and acoustic emission response of sandstone during loading process: phenomenon and mechanism. *Eng Geol* 294:106386
- Li X, Peng K, Peng J, Hou D (2021c) Experimental investigation of cyclic wetting–drying effect on mechanical behavior of a medium-grained sandstone. *Eng Geol* 293:106335
- Liang H, Fu Y (2020) Fracture properties of sandstone degradation under the action of drying–wetting cycles in acid and alkaline environments. *Arab J Geosci* 13(2):1–8
- Lin Q, Cao P, Cao R, Fan X (2019) Acoustic emission characteristics during rock fragmentation processes induced by disc cutter under different water content conditions. *Appl Sci* 9(1):194
- Liu W, Zhang Z (2020) Experimental characterization and quantitative evaluation of slaking for strongly weathered mudstone under cyclic wetting–drying condition. *Arab J Geosci* 13(2):1–8
- Liu S, Wu L, Zhang Y, Chen Q (2010) Change feature of infrared radiation from loaded damp rock. *J Northeast Univ* 31(2):1034–1038
- Liu X, Wang Z, Fu Y, Yuan W, Miao L (2016) Macro/microtesting and damage and degradation of sandstones under dry–wet cycles. *Adv Mater Sci Eng* 2016:1–16
- Liu X, Jin M, Li D, Zhang L (2018) Strength deterioration of a Shaly sandstone under dry–wet cycles: a case study from the Three Gorges Reservoir in China. *Bull Eng Geol Environ* 77(4):1607–1621
- Liu X, Wu L, Zhang Y, Liang Z, Yao X, Liang P (2019) Frequency properties of acoustic emissions from the dry and saturated rock. *Environ Earth Sci* 78(3):1–17
- Liu C, Cheng Y, Jiao Y, Zhang G, Zhang W, Ou G, Tan F (2021) Experimental study on the effect of water on mechanical properties of swelling mudstone. *Eng Geol* 295:106448
- Liu ZY, Wang G, Li JZ, Li HZ, Zhao HF, Shi HW, Lan JL (2022) Water-immersion softening mechanism of coal rock mass based on split Hopkinson pressure bar experiment. *Int J Coal Sci Technol* 9(1):61
- Lu G, Crandall D, Bunker AP (2021) Observations of breakage for transversely isotropic shale using acoustic emission and X-ray computed tomography: effect of bedding orientation, pre-existing weaknesses, and pore water. *Int J Rock Mech Min Sci* 139:104650
- Luo Y (2020) Influence of water on mechanical behavior of surrounding rock in hard-rock tunnels: an experimental simulation. *Eng Geol* 277:105816
- Luo J, Tang H, Sui Z (2021) Hydrochemistry of coal samples in water immersion process. *Sci Technol Eng* 21(29):12431–12437
- Lyu Q, Wang K, Hu C, Dick JM, Shi J, Tan J (2022) Experimental study on the mechanical properties of shale after long-term of immersion in fracturing fluids with different pH. *Rock Mech Rock Eng* 55:5047–5061
- Ma Q, Yu P, Yuan P (2018) Experimental study on the influence of dry wet cycle on creep characteristics of deep siltstone. *J Rock Mech Eng* 37(3):593–600
- Ma D, Duan H, Zhang J, Feng X, Huang Y (2021) Experimental investigation of creep–erosion coupling mechanical properties of water inrush hazards in fault fracture rock masses. *Chin J Rock Mech Eng* 40(9):1751–1763
- Ma D, Duan HY, Zhang JX, Bai HB (2022) A state-of-the-art review on rock seepage mechanism of water inrush disaster in coal mines. *Int J Coal Sci Technol* 9(1):50. <https://doi.org/10.1007/s40789-022-00525-w>
- Miao C, Yang L, Xu Z, Yang K, Sun X, Jiang M, Zhao W (2021) Experimental study on strength softening behaviors and micro-mechanisms of sandstone based on nuclear magnetic resonance. *Chin J Rock Mech Eng* 40(11):2189–2198
- Momeni A, Hashemi SS, Khanlari GR, Heidari M (2017) The effect of weathering on durability and deformability properties of granitoid rocks. *Bull Eng Geol Environ* 76(3):1037–1049
- Noël C, Baud P, Violay M (2021) Effect of water on sandstone’s fracture toughness and frictional parameters: brittle strength constraints. *Int J Rock Mech Min Sci* 147:104916

- Özbek A (2014) Investigation of the effects of wetting–drying and freezing–thawing cycles on some physical and mechanical properties of selected ignimbrites. *Bull Eng Geol Environ* 73(2):595–609
- Qin Z, Chen X, Fu H (2018) Damage features of altered rock subjected to drying–wetting cycles. *Adv Civ Eng* 2018:1–10
- Rabat Á, Cano M, Tomás R, Tamayo ÁE, Alejano LR (2020) Evaluation of strength and deformability of soft sedimentary rocks in dry and saturated conditions through needle penetration and point load tests: a comparative study. *Rock Mech Rock Eng* 53(6):2707–2723
- Ranjith PG, Jasinge D, Song J, Choi SK (2008) A study of the effect of displacement rate and moisture content on the mechanical properties of concrete: use of acoustic emission. *Mech Mater* 40(6):453–469
- Shen R, Li H, Wang E, Chen T, Li T, Tian H, Hou Z (2020) Infrared radiation characteristics and fracture precursor information extraction of loaded sandstone samples with varying moisture contents. *Int J Rock Mech Min Sci* 130:104344
- Song C, Ji H, Liu Z, Zhang Y, Wang H, Tan J (2019) Experimental study on acoustic emission characteristics of weakly cemented rock under dry wet cycle. *J Min Saf Eng* 36(04):812–819
- Song H, Zhao Y, Jiang Y, Du W (2020) Experimental investigation on the tensile strength of coal: consideration of the specimen size and water content. *Energies* 13(24):6585
- Sun Q, Zhang Y (2019) Combined effects of salt, cyclic wetting and drying cycles on the physical and mechanical properties of sandstone. *Eng Geol* 248:70–79
- Sun X, Xu H, Zheng L, He M, Gong W (2016) An experimental investigation on acoustic emission characteristics of sandstone rockburst with different moisture contents. *Sci China Technol Sci* 59(10):1549–1558
- Sun H, Ma L, Fu Y, Han J, Liu S, Chen M, Tian F (2021a) Infrared radiation test on the influence of water content on sandstone damage evolution. *Infrared Phys Technol* 118:103876
- Sun X, Miao C, Jiang M, Zhang Y, Yang L, Guo B (2021b) Experimental and theoretical study on creep of sandstone with different moisture content based on modified Nishihara model. *Chin J Rock Mech Eng* 40(12):2411–2420
- Talesnick M, Shehadeh S (2007) The effect of water content on the mechanical response of a high-porosity chalk. *Int J Rock Mech Min Sci* 44(4):584–600
- Tang S (2018) The effects of water on the strength of black sandstone in a brittle regime. *Eng Geol* 239:167–178
- Tang SB, Yu CY, Heap MJ, Chen PZ, Ren YG (2018) The influence of water saturation on the short-and long-term mechanical behavior of red sandstone. *Rock Mech Rock Eng* 51(9):2669–2687
- Tang C, Yao Q, Xu Q, Shan C, Xu J, Han H, Guo H (2021) Mechanical failure modes and fractal characteristics of coal samples under repeated drying-saturation conditions. *Nat Resour Res* 30(6):4439–4456
- Topal T, Sözmen B (2003) Deterioration mechanisms of tuffs in Midas monument. *Eng Geol* 68(3–4):201–223
- Ukpai SN (2021) Stability analyses of dams using multidisciplinary geoscience approach for water reservoir safety: case of Mpu Damsite, Southeastern Nigeria. *Bull Eng Geol Environ* 80(3):2149–2170
- Verstrynge E, Adriaens R, Elsen J, Van Balen K (2014) Multi-scale analysis on the influence of moisture on the mechanical behavior of ferruginous sandstone. *Constr Build Mater* 54:78–90
- Wang Y, Huang W, Li Z, Chang L, Li D, Chen R, Lv B (2021) Small furnace for the small angle X-ray scattering (SAXS) and wide angle X-ray scattering (WAXS) characterization of the high temperature carbonization of coal. *Instrum Sci Technol* 49(4):445–456
- Wu B, Liu K, Guo D (2020a) Study on the change law of mechanical properties of gritstone under the influence of mine water. *J Min Sci Technol* 5(6):632–637
- Wu B, Wang W, Guo D (2020b) Strength damage and AE characteristics of fractured sandstone under the influence of water intrusion times. *J Min Saf Eng* 37(5):1054
- Xiao W, Zhang D, Wang X (2020) Experimental study on progressive failure process and permeability characteristics of red sandstone under seepage pressure. *Eng Geol* 265:105406
- Xie K, Jiang D, Sun Z, Chen J, Zhang W, Jiang X (2018) NMR, MRI and AE statistical study of damage due to a low number of wetting–drying cycles in sandstone from the three gorges reservoir area. *Rock Mech Rock Eng* 51(11):3625–3634
- Yang X, Wang J, Hou D, Zhu C, He M (2018) Effect of dry-wet cycling on the mechanical properties of rocks: a laboratory-scale experimental study. *Processes* 6(10):199
- Yao Q, Chen T, Ju M, Liang S, Liu Y, Li X (2016) Effects of water intrusion on mechanical properties of and crack propagation in coal. *Rock Mech Rock Eng* 49(12):4699–4709
- Yao Q, Chen T, Tang C, Sedighi M, Wang S, Huang Q (2019a) Influence of moisture on crack propagation in coal and its failure modes. *Eng Geol* 258:105156
- Yao Q, Hao Q, Chen X, Zhou B, Fang J (2019b) Design on the width of coal pillar dam in coal mine groundwater reservoir. *J China Coal Soc* 44(3):891–899
- Yao Q, Tang C, Xia Z, Liu X, Zhu L, Chong Z, Hui X (2020a) Mechanisms of failure in coal samples from underground water reservoir. *Eng Geol* 267:105494
- Yao Q, Wang W, Zhu L, Xia Z, Tang C, Wang X (2020b) Effects of moisture conditions on mechanical properties and AE and IR characteristics in coal–rock combinations. *Arab J Geosci* 13(14):1–15
- Yao W, Li C, Zhan H, Zhou JQ, Criss RE, Xiong S, Jiang X (2020c) Multiscale study of physical and mechanical properties of sandstone in three Gorges reservoir region subjected to cyclic wetting–drying of yangtze river water. *Rock Mech Rock Eng* 53(5):2215–2231
- Yu C, Tang S, Duan D, Zhang Y, Liang Z, Ma K, Ma T (2019) The effect of water on the creep behavior of red sandstone. *Eng Geol* 253:64–74
- Zhang Z, Jiang Q, Zhou C, Liu X (2014) Strength and failure characteristics of Jurassic Red-Bed sandstone under cyclic wetting–drying conditions. *Geophys J Int* 198(2):1034–1044
- Zhang N, Wang S, Yan C, Gao J, Guo R, Wang H (2019) Pore structure evolution of hydration damage of mudstone based on NMR technology. *J China Coal Soc* 44(S1):110–117
- Zhang W, Zhang D, Zhao J (2021) Experimental investigation of water sensitivity effects on microscale mechanical behavior of shale. *Int J Rock Mech Min Sci* 145:104837
- Zhao Y, Liu S, Elsworth D, Jiang Y, Zhu J (2014) Pore structure characterization of coal by synchrotron small-angle X-ray scattering and transmission electron microscopy. *Energy Fuels* 28(6):3704–3711
- Zhao Y, Xue S, Han S, Chen Z, Liu S, Elsworth D, Chen D (2017a) Effects of microstructure on water imbibition in sandstones using X-ray computed tomography and neutron radiography. *J Geophys Res Solid Earth* 122(7):4963–4981
- Zhao Z, Yang J, Zhang D, Peng H (2017b) Effects of wetting and cyclic wetting–drying on tensile strength of sandstone with a low clay mineral content. *Rock Mech Rock Eng* 50(2):485–491
- Zhao Z, Yang J, Zhou D, Chen Y (2017c) Experimental investigation on the wetting-induced weakening of sandstone joints. *Eng Geol* 225:61–67
- Zhao Y, Ren S, Jiang D, Liu R, Wu J, Jiang X (2018a) Influence of wetting–drying cycles on the pore structure and mechanical

- properties of mudstone from Simian Mountain. *Constr Build Mater* 191:923–931
- Zhao Y, Xue S, Han S, He L, Chen Z (2018b) Characterization of unsaturated diffusivity of tight sandstones using neutron radiography. *Int J Heat Mass Transf* 124:693–705
- Zhao Z, Guo T, Ning Z, Dou Z, Dai F, Yang Q (2018c) Numerical modeling of stability of fractured reservoir bank slopes subjected to water–rock interactions. *Rock Mech Rock Eng* 51(8):2517–2531
- Zhao Y, Peng L, Liu S, Cao B, Sun Y, Hou B (2019a) Pore structure characterization of shales using synchrotron SAXS and NMR cryoporometry. *Mar Pet Geol* 102:116–125
- Zhao Y, Wu Y, Han S, Xue S, Fan G, Chen Z, El Abd A (2019b) Water sorptivity of unsaturated fractured sandstone: fractal modeling and neutron radiography experiment. *Adv Water Resour* 130:172–183
- Zhao F, Sun Q, Zhang W (2020) Combined effects of salts and wetting–drying cycles on granite weathering. *Bull Eng Geol Environ* 79(7):3707–3720
- Zhao B, Li Y, Huang W, Yang J, Sun J, Li W, Zhang L (2021) Mechanical characteristics of red sandstone under cyclic wetting and drying. *Environ Earth Sci* 80(22):1–12
- Zhong C, Zhang Z, Ranjith PG, Lu Y, Choi X (2019) The role of pore water plays in coal under uniaxial cyclic loading. *Eng Geol* 257:105125
- Zhou Z, Cai X, Chen L, Cao W, Zhao Y, Xiong C (2017) Influence of cyclic wetting and drying on physical and dynamic compressive properties of sandstone. *Eng Geol* 220:1–12
- Zhou Z, Cai X, Ma D, Cao W, Chen L, Zhou J (2018a) Effects of water content on fracture and mechanical behavior of sandstone with a low clay mineral content. *Eng Fract Mech* 193:47–65
- Zhou Z, Cai X, Ma D, Chen L, Wang S, Tan L (2018b) Dynamic tensile properties of sandstone subjected to wetting and drying cycles. *Constr Build Mater* 182:215–232
- Zhou Z, Xiong C, Cai X, Zhao Y, Li X, Du K (2018c) Mechanical and infrared radiation properties of sandstone with different water contents under uniaxial compression. *J Cent South Univ (sci Technol)* 49(5):1189–1196
- Zhu J, Deng J, Chen F, Huang Y, Yu Z (2020) Water saturation effects on mechanical and fracture behavior of marble. *Int J Geomech* 20(10):04020191
- Zhu J, Deng J, Chen F, Ma Y, Yao Y (2021) Water-weakening effects on the strength of hard rocks at different loading rates: an experimental study. *Rock Mech Rock Eng* 54(8):4347–4353

Publisher's Note Springer Nature remains neutral with regard to jurisdictional claims in published maps and institutional affiliations.